COLLOID CHEMISTRY
AND ELECTROCHEMISTRY

Computer Modeling of Lithium Intercalation and Deintercalation in a Silicene Channel

A. E. Galashev[a,*] and K. A. Ivanichkina[a]

[a] Institute of High-Temperature Electrochemistry, Ural Branch,
Russian Academy of Sciences, Yekaterinburg, 620137 Russia
e-mail: galashev@ihte.uran.ru

Abstract—The sequential intercalation/deintercalation of Li$^+$ in a silicene channel was studied by molecular dynamics. The maximum density of 0.063 Li atoms per 1 Si atom in the channel was achieved when the slit volume increased by 24%. A flat 13-atomic lithium cluster was found to form at an early stage of intercalation, which was destroyed further during the process. The character of the motion of the Li$^+$ ion during the cycling was analyzed. The self-diffusion coefficients of lithium atoms in both processes were determined. The number of Li atoms leaving the channel and their residence time in the channel after the appearance of the next ion during deintercalation in the system was determined.

Recently obtained silicon in a 2D configuration with a nonplanar atomic lattice called "silicene" is of considerable interest due to its unique properties and compatibility with existing semiconductor technologies [1]. Silicene has a "corrugated" structure with a rather low height of surface bending [2–4]. One of the remarkable properties of silicon is its ability to hold a record number of lithium atoms (4.4 Li atoms per Si atom) during intercalation [5]. In this case, a "chemical compound" Li$_{4.4}$Si forms in bulk silicon. The composition of the Li–Si compound was determined by spectrometry and gravimetric analysis. The theoretical capacity of a silicon anode exceeds that of a graphite electrode 11.3-fold. Therefore, silicene is one of the best candidates for the anode material for lithium-ion batteries of a new generation [6]. A transition from crystalline silicon to nanoparticles and thin Si films as anode material offers a solution to the problem of silicon anode breakage as a result of lithiation/delithiation cycles [7]. The use of double-layer silicene for this purpose is especially promising because it is easier to obtain than monolayer silicene [8]. It is assumed that silicene, like functionalized graphene sheets, can be used as electrodes, giving high electric capacity [9]. The capacity of the channel (slit-like pore) can be regarded as an addition to the anode capacity obtained by using the outer surface of silicene sheets for anodic processes.

The goal of this study was to investigate the occupancy of the silicene channel with lithium during the sequential introduction of its ions in the channel under the action of an electric field and to study the reverse process of forced withdrawal of ions from the channel.

COMPUTER MODEL

The calculations were performed by the molecular dynamics method. The Tersoff potential [10] was taken as a basis for representation of interactions in silicene:

$$V_{ij} = f_C(r_{ij})[A\exp(-\lambda^{(1)}r_{ij}) - Bb_{ij}\exp(-\lambda^{(2)}r_{ij})],$$

$$f_C(r_{ij}) = \begin{cases} 1, & r_{ij} < R^{(1)} \\ \dfrac{1}{2} + \dfrac{1}{2}\cos[\pi(r_{ij} - R^{(1)})/(R^{(2)} - R^{(1)})], \\ & R^{(1)} < r_{ij} < R^{(2)} \\ 0, & r_{ij} > R^{(2)}, \end{cases}$$

$$b_{ij} = (1 + \beta^n \xi_{ij}^{n_i})^{-1/(2n)}, \qquad (1)$$

$$\xi_{ij} = \sum_{k \neq i,j} f_C(r_{ij})g(\theta_{ijk}),$$

$$g(\theta_{ijk}) = 1 + \frac{c^2}{d^2} - \frac{c^2}{[d^2 + (h - \cos\theta_{ijk})^2]}.$$

Here, the indices i, j, k denote the silicon atoms; r_{ij} is the i–j bond length; θ_{ijk} is the angle between the i–j and j–k bonds. The parameters of this potential and the electric charge of the Li$^+$ ion are given in Table 1.

Table 1. Parameters of the Tersoff potential for representation of Si−Si interactions [10]

A, eV	B, eV	λ_1, nm^{-1}	λ_2, nm^{-1}	n	h
1830.8	471.18	2.4799	1.7322	0.78734	−0.59825
c	d	$R^{(1)}$, nm	$R^{(2)}$, nm	β	q, C
1.0039×10^5	16.217	0.27	0.30	1.1×10^{-6}	1.6×10^{-19}

The interactions between the Si atoms belonging to different silicene sheets was described by the Morse potential [11]:

$$V(r_{ij}) = D_e(\exp[-2\alpha(r_{ij} - r_e)] \\ - 2\exp[-\alpha(r_{ij} - r_e)]). \quad (2)$$

Here, D_e is the depth of the potential well, α is the rigidity parameter, and r_e is the equilibrium bond length.

The Morse potential was used for describing the intersheet Si−Si and all Li−Si interactions with the parameters: $D_e^{Si-Si} = 0.2274$ eV, $\alpha^{Si-Si} = 15.390$ nm^{-1} $r_e^{Si-Si} = 0.4499$ nm; and $D_e^{Li-Si} = 0.30932$ eV, $\alpha^{Li-Si} = 11.6445$ nm^{-1}, and $r_e^{Li-Si} = 0.36739$ nm [8, 12, 13]. The equations of motion were numerically solved by the Runge−Kutta fourth-order method at a time step of $\Delta t = 1 \times 10^{-16}$ s.

In this paper, we consider the case of reconstructing a surface of 4 × 4. A single cell of this silicene structure contains 18 Si atoms. Six Si atoms of the single cell are displaced in a direction perpendicular to the surface by a distance of 0.064 nm, and the remaining Si atoms lie on the same (initial) plane. This structure of a silicene sheet is similar to the silicene surface observed on an Ag(111) substrate [14]. In the upper sheet, the atoms are shifted upward from the initial surface of two-layer silicene, while in the lower sheet the atoms are shifted downward. The introduction of Li$^+$ ions in the silicene channel was studied given a gap of $h_g = 0.75$ nm between the silicene sheets. It was previously determined [5] that with this gap in the absence of deformation created by lithium atoms in the channel, a single Li$^+$ ion can reside in the silicene channel for 100 ps at an electric field with a strength of $E = 10^3$ V/m. At this empirically selected E value, the ion could move through the channel and be fixed on one of the sheets.

Note that for a real silicon anode in the case of using solid oxide electrolyte (LIPON) with a thickness of ~500 μm at a generated voltage of 1.5 V, the electric field strength is 3×10^3 V/m [15], which is in satisfactory agreement with the E value in this work. The

edges of the silicene sheets were fixed. This was achieved due to the fact that the atoms that formed the edges of the sheets were fixed. Fixing the positions of the edge atoms makes it possible to avoid the bending of the sheets due to the appearance of the resulting torque in the case of applying the Tersoff potential to two-dimensional systems [16−18]. The sheet of perfect silicene was 4.8 × 4.1 nm in size (taking into account the size of Si atoms) and contained 300 atoms.

The initial distribution of particle velocities was set using the Maxwell distribution corresponding to a temperature of 300 K. The calculations were performed in the *NVT* ensemble. Outside the simulated system, a force field acted on all sides, allowing the number of particles in the model to be kept constant. This field was created by the Lennard-Jones potential with the parameters: σ = 0.1 nm, ε = 1 eV. The repulsion of particles produced by this potential was at a distance of $r > 0.25$ nm from the edges of the silicene sheets. Before launching the first ion into the channel, the system was preliminarily relaxed at 300 K for 1.0 million time steps. This temperature of the system was also maintained during the subsequent (main) simulation.

The modeling of intercalation consisted in the intermittent single or double emission of Li$^+$ ions from points with random y coordinates located on a line with constant coordinates $x = 0.55$ nm, $z = 0.375$ nm. In other words, the line of initial points was located near the entrance to the channel with a slight shift inward at a height of $h_g/2$. The end points of the line were located inside the channel at a distance of 0.2 nm from the y coordinates of the terminal atoms of silicene that limited the sheet length along the x direction. The ion began to move in the x direction and moved for 100 000 time steps (10 ps) under the action of a constant electric field with a strength of 10^3 V/m. The ion remained in the channel throughout its lifetime (10 ps) until the channel was ultimately filled with lithium because it could not overcome the barrier created by the attracting interaction of other atoms. It was assumed that the Li$^+$ ion turned into a lithium atom after 10 ps due to charge redistribution. The difference in the interaction (with the field) between the lithium ion and atom consisted only in the presence of a charge of $+1e$ on the ion. The character of its interaction with other atoms (Si and Li) did not change. A new Li$^+$ ion was launched into the channel every 10 ps. This procedure was repeated as long as the ions could find a place in the channel. At first, there was only one ion in the system at each moment of time. After 24 Li atoms appeared in the channel, however, the subsequent attempts to introduce lithium in the channel were made while simultaneously launching two Li$^+$ ions into the channel, which interacted with each other according to Coulomb's law. As a result, the number of lithium atoms in the channel was brought to 38.

Lithium deintercalation was performed by changing the direction of electric field strength to the opposite and significantly increasing E (to 10^5 V/m). The order of appearance of ions in the system was also reverse, and the lifetime of the ion was increased to 20 ps. These changes allowed the ionized Li atoms to successfully overcome the potential barrier caused by the interatomic interaction under the action of the field. Deintercalation in the model had higher discreteness than intercalation. This is due to the fact that the Li$^+$ ion did not leave the channel alone, but was always accompanied by 2 to 10 lithium atoms, and the number of moving Li atoms at the initial stage of deintercalation was greater than at its final stage.

The self-diffusion coefficient was calculated in terms of the mean square displacement of atoms $\left\langle [\Delta \mathbf{r}(t)]^2 \right\rangle$:

$$D = \lim_{t \to \infty} \frac{1}{2\Gamma t} \left\langle [\Delta \mathbf{r}(t)]^2 \right\rangle, \qquad (3)$$

where $\Gamma = 3$ is the dimensionality of the space, and $\langle ... \rangle$ is the time averaging. The coefficient D was calculated on the time interval of 2 ps; this allowed averaging of two to five dependences $\left\langle [\Delta \mathbf{r}(t)]^2 \right\rangle_{t_0}$ calculated for different initial moments of time t_0 chosen during the lifetime of one ion. In each interval taken into account during the calculation of $\left\langle [\Delta \mathbf{r}(t)]^2 \right\rangle$, the ion resided for at least 1 ps in the channel. Thus, each lifetime of the ion corresponds to its own D value for Li atoms.

The calculations were performed using the LAMMPS program [19] for parallel MD computations on a hybrid cluster-type computer URAN at the Institute of Mathematics and Mechanics, Ural Branch, Russian Academy of Sciences.

RESULTS AND DISCUSSION

To show the maximum capacity of the silicene channel, 52 tests were performed. Each test was a 10-ps MD calculation. The result of the study of the intercalation process was the introduction of only 38 Li$^+$ ions in the channel. After these successful attempts, another 14 tests were performed, which ended with finding the Li$^+$ ion outside the channel. The silicene channel filled with 38 lithium atoms is shown in Fig. 1. The lithium atoms located outside the cluster and the ion are not shown in the figure. The accommodation of Li atoms in the channel is irregular and nonuniform. The silicene sheets are bent outward. This deformation led to an increase in the initial volume of the system by 26%. The volume of the slit space V was calculated by dividing the area of one of the silicene sheets into equal areas ΔS_i around the sites of 300 Si atoms and by determining the heights h_i for
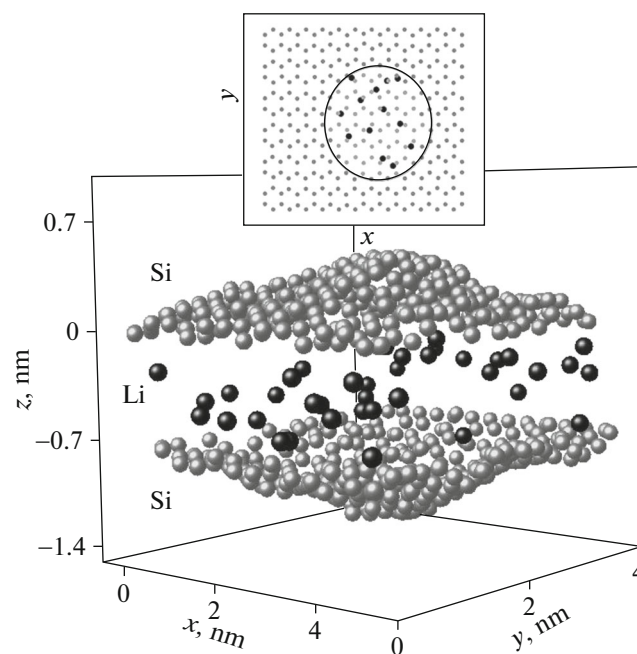

Fig. 1. Accommodation of 38 lithium atoms in a silicene channel obtained by the moment of time of 0.52 ns. Insert: *xy* projection of the upper silicene sheet with an indicated site of the flat 13-atomic lithium cluster corresponding to the moment of time of 0.15 ns.

these sites as the differences of the z coordinates of the corresponding atoms of the upper and lower sheets. Then V is determined as $V \approx \sum_{i=1}^{300} \Delta S_i h_i$, and $\Delta V = V_2 - V_1$, where V_1 and V_2 are the initial and final volumes of the interslit space, respectively.

After deintercalation we performed an additional calculation with a duration of 100 ps with an empty channel (without lithium) to examine the possibility of correcting its shape. As a result of this calculation, the bulging of silicene sheets decreased, and the volume of the system was reduced by only 5% of the maximum value obtained during lithium intercalation. In other words, the initial shape of the channel was not restored.

The insert of Fig. 1 shows the *xy* projection of the upper sheet of silicene, in which the region (circle) with the formed 13-atomic Li cluster is shown. The cluster formation was determined based on both the energy and geometric criteria. According to the first criterion, the energy of interacting atomic pairs in a cluster should be negative, at least 10% of the depth of the corresponding potential well. The second criterion ensured that the atoms belonged to the cluster when the distance between them did not exceed 0.3 nm, which is typical of the forming pairs of Li atoms [20]. A cluster of 13 Li atoms formed when there were 15 Li atoms in the channel and collapsed in ~40 ps (at $N = $ 19). As the model used does not provide for chemical
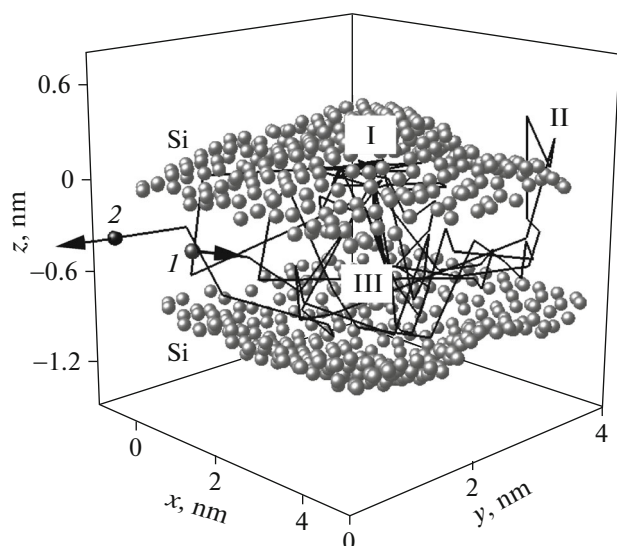
Fig. 2. Trajectory of the motion of the lithium ion (atom) during the intercalation/deintercalation cycle including regions I−III described in the text; *1* and *2* are the locations of the Li$^+$ ion at the moment of entering and exiting the channel, respectively.

Fig. 3. Self-diffusion coefficient D of lithium atoms depending on their number N in the silicene channel; intercalation (left part) and deintercalation (right part); (*1*) dependence $D(N)$ obtained in the MD model and (*2*) approximation of the MD calculated data by a third-degree polynomial.
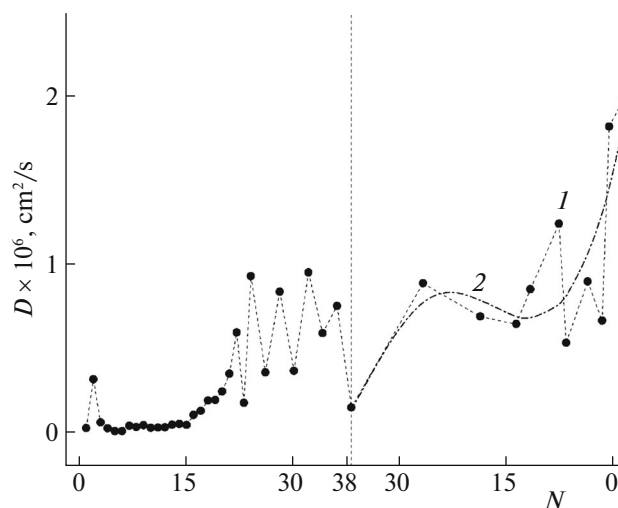
bonding, the addition of lithium to the silicene surface occurred due to physical adsorption. As a result of our study, it was found that in the slit pore formed by two silicene sheets (together containing 600 Si atoms), 38 Li atoms are deposited and preserved. Thus, we observed the physical adsorption of lithium in the slit pore in a ratio of 1 Li per 15.7 Si.

The trajectory of the motion (at 0.68 ns) of one of the Li atoms belonging to the cluster and entering second (as a Li$^+$ ion) in the channel is shown in Fig. 2. The trajectory is divided into regions (denoted by Roman numerals), where the ion (atom) shows the characteristic features of its behavior.

Regions I and II refer to ion intercalation, and region III refers to deintercalation. The ion that enters the channel moves under the action of the external electric field and interacts with the atoms of both the upper and lower silicene sheets, as a result of which it acquires an oscillating trajectory.

Region I reflects the time interval of 0.19 ns. During this period of time, a cluster of 13 Li atoms formed and even started to be destroyed. The oscillations of this atom in the cluster occurred mainly in the horizontal direction, and the cluster was a flat formation.

Region II corresponds to the time interval of ~0.33 ns. As the number of Li atoms in the channel increases, the cluster destruction continues, and the atom in question moves closer to the exit from the channel, performing significant, mainly vertical, vibrations. However, the persisting attraction to silicon atoms did not allow the Li atom to leave the channel.

Region III includes the trajectory of the selected Li atom during deintercalation and is characterized by duration of 0.16 ns. When leaving the channel, the ions entrain some atoms together with them, introducing a strong perturbation and changing the character of motion of the atom in different parts of the channel.

Intercalation, especially at $N \le 15$, takes place at lower D values for Li atoms than the reverse process (Fig. 3). At $N > 15$, D continues to increase even after the destruction of the 13-atomic cluster up to $N = 22$. The fluctuations of D at $22 \le N \le 38$ characterize the structural rearrangements that lead to the formation of an irregular nonuniform packing of Li atoms in the channel. An increase in the D coefficient at the final stage of intercalation is associated with the faster displacement of Li atoms located closer to the edges of the silicene sheets.

The D coefficient also increases during deintercalation due to a decrease in the number of lithium atoms in the channel (dependence *1*, Fig. 3). Dependence *2* in Fig. 3 reflects the approximation of the $D(N)$ dependence by a third-degree polynomial. At each interval of 20 ps, the number of Li atoms in the channel decreases (ΔN); the largest value of ΔN (10) is observed at the first step of deintercalation, when the density of Li atoms in the channel is maximum. The highest increase in D occurs at the first and last but one deintercalation steps. In the former case, this is due to the large number of Li atoms removed from the channel, which acquire a significant rate on leaving the channel; in the latter case, this is due to the freer and faster motion of the few Li atoms remaining in the channel.
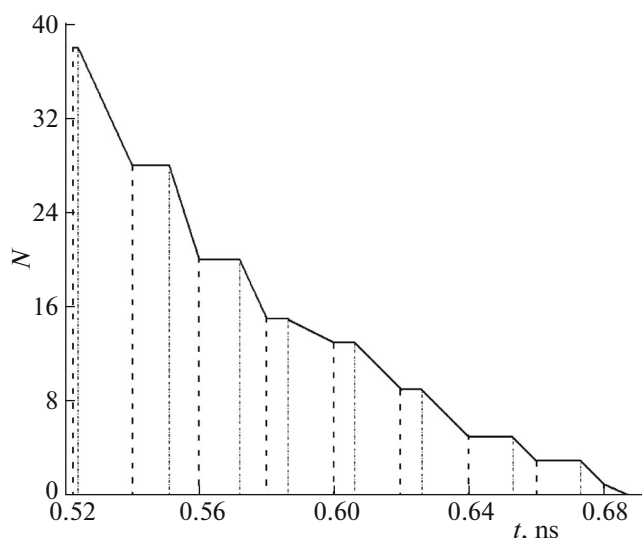
Fig. 4. Time dependence of the number of lithium atoms in the silicene channel during the deintercalation. At $t > 0.68$ ns, the last Li^+ ion is removed from the channel.

The deintercalation starts from the moment of time of 0.520 ns and ends by 0.688 ns (Fig. 4). The region of this process in Fig. 4 is divided by the vertical dashed lines into equal portions of 20 ps and vertical dash-dotted lines that determine the time at which the first atom leaves the channel in the given region of deintercalation. The horizontal sections of the $N(t)$ dependence show that the initial number of Li atoms is preserved in each 20-ps interval during deintercalation. The sloping regions characterize the decrease in the initial N value for the selected interval and determine the number (ΔN) of Li atoms leaving the channel during the lifetime of a particular Li^+ ion. The shortest period of the presence (4 ps) of a constant number of Li atoms in the channel is observed in the first interval, where the number of Li atoms leaving the channel is maximum ($\Delta N = 10$). The last but one interval is characterized by the longest (14 ps) stay of the constant number of Li atoms in the channel and one of the lowest values of ΔN (2). The last Li^+ ion exits the channel alone.

The modeling performed in this study simulates the lithium filling of a hardly accessible section of a thin-film silicon anode. The lithium ion passes through three specific regions of characteristic displacements in the channel during the anode cycle under study. During the step-by-step deintercalation determined by the lifetime of the ion, not only the Li^+ ion but also a whole group of Li atoms leaves the channel. The D coefficient increased significantly as the channel was liberated from lithium. Thus, it was shown that silicene can be used as the anode material of the lithium-ion battery. The increase in the anode capacity due to the presence of a slit-like silicene pore in it was studied.

ACKNOWLEDGMENTS

REFERENCES

1. T.-T. Jia, M.-M. Zheng, X.-Y. Fan, et al., J. Phys. Chem. C **119**, 20747 (2015).
2. S. Cahangirov, M. Topsakal, E. Akturk, et al., Phys. Rev. Lett. **102**, 236804 (2009).
3. K. Takeda and K. Shiraishi, Phys. Rev. B **50**, 14916 (1994).
4. M. Houssa, G. Poutois, V. V. Afanasev, and A. Stesmans, Appl. Phys. Lett. **97**, 112106 (2010).
5. A. E. Galashev, Yu. P. Zaikov, and R. G. Vladykin, Russ. J. Electrochem. **52**, 966 (2016).
6. A. E. Galashev, K. A. Ivanichkina, A. S. Vorob'ev, and O. R. Rakhmanova, Phys. Solid State **59**, 1242 (2017).
7. A. E. Galashev and K. A. Ivanichkina, Russ. J. Phys. Chem. A **91**, 2244 (2017).
8. O. R. Rakhmanova and A. E. Galashev, Russ. J. Phys. Chem. A **91**, 921 (2017).
9. J. Xiao, D. Mei, X. Li, et al., Nano Lett. **11**, 5071 (2011).
10. J. Tersoff, Phys. Rev. B **39**, 5566 (1989).
11. R. Yu, P. Zhai, G. Li, and L. Liu, J. Electron. Mater. **41**, 1465 (2012).
12. E. C. Angel, J. S. Reparaz, J. Gomis-Bresco, et al., APL Mater. **2**, 012113 (2014).
13. S. K. Das, D. Roy, and S. Sengupta, J. Phys. F: Met. Phys. **7**, 5 (1977).
14. K. Kawahara, T. Shirasawa, R. Arafune, et al., Surf. Sci. **623**, 25 (2014).
15. K. S. Jones, State of Solid-State Batteries. http://ceramics.org/wp-content/uploads/2011/08/energy-ss-batteries-jones.pdf.
16. A. E. Galashev and Yu. P. Zaikov, Russ. J. Phys. Chem. A **89**, 2243 (2015).
17. A. E. Galashev and V. A. Polukhin, Phys. Solid State **55**, 1733 (2013).
18. A. E. Galashev, Tech. Phys. **59**, 467 (2014).
19. S. Plimpton, J. Comp. Phys. **117**, 1 (1995).
20. A. A. Kuzubov, P. V. Avramov, S. G. Ovchinnikov, S. A. Varganov, and F. N. Tomilin, Phys. Solid State **43**, 1794 (2001).

Translated by L. Smolina